

# Multiparametric MRI analysis for the evaluation of MR-guided High Intensity Focused Ultrasound treatment

Stefanie Hectors<sup>1</sup>, Igor Jacobs<sup>1</sup>, Edwin Heijman<sup>2</sup>, Jochen Keupp<sup>3</sup>, Monique Berben<sup>2</sup>, Gustav Strijkers<sup>1,4</sup>, Holger Gröll<sup>1,2</sup>, and Klaas Nicolay<sup>1</sup>

<sup>1</sup>Biomedical NMR, Department of Biomedical Engineering, Eindhoven University of Technology, Eindhoven, Netherlands, <sup>2</sup>Oncology Solutions, Philips Research Europe, Eindhoven, Netherlands, <sup>3</sup>Tomographic Imaging Systems, Philips Research Europe, Hamburg, Germany, <sup>4</sup>Biomedical Engineering and Physics, Academic Medical Center, University of Amsterdam, Amsterdam, Netherlands

**Introduction** For the clinical application of High Intensity Focused Ultrasound (HIFU) treatment of malignant lesions, accurate treatment evaluation is of key importance. In a previous study, in which the HIFU treatment was performed outside the high-field preclinical MR scanner, we have shown that successfully HIFU-treated tumor tissue can be identified using a multiparametric MRI analysis based on  $T_1$ ,  $T_2$  and apparent diffusion coefficient (ADC) data<sup>1</sup>. In subsequent studies, we have demonstrated that amide proton transfer (APT) imaging<sup>2</sup> and  $T_{1\rho}$  mapping<sup>3</sup> are additional MRI methods that are sensitive to HIFU-induced tissue changes. In the present study, we have employed a multiparametric MRI protocol combining all these promising MRI methods to evaluate HIFU treatment of rat tumors in a clinical 3T MR-HIFU system, which facilitated real-time temperature monitoring during treatment. Cluster analysis was performed on the multiparametric MRI data and the optimal set of MR parameters to identify successfully treated tumor was determined by quantitative comparison with histology.

**Materials and Methods** 9L glioma tumor-bearing (hind limb) Fischer 344 rats were subjected to MRI before (n=12), directly after (n=12) and 3 days after (n=6) HIFU treatment. In addition, a non-treated control group (n=6) was included. All animals were positioned in a rat MR-HIFU setup<sup>4</sup> placed on the tabletop of a clinical Philips 3T Sonallevé MR-HIFU system. Partial tumor ablation (4 mm diameter treatment cell) was performed with an acoustic power of 35 W and duration of 90 s. MR thermometry (PRFS method), from which thermal dose maps were calculated, was performed during treatment. The multiparametric MRI protocol consisted of quantitative  $T_1$ ,  $T_2$ , ADC, APT,  $T_{1\rho}$  and dynamic contrast-enhanced MRI (DCE-MRI) acquisitions. DCE-MRI was only performed after ablation. After the last MR experiments, tumors were marked, excised and sliced according to the orientation of the central MRI slice. NADH-diaphorase staining was performed to determine non-viable tumor fractions. K-means clustering with 4 clusters and all possible feature vectors (i.e. all different combinations of MR parameters) was performed on the MR parameter values in the tumor (excluding the DCE-MRI results because of absence of DCE-MRI data before treatment). Clusters in which the fraction of pixels significantly increased after MR-HIFU treatment were classified as non-viable. The optimal feature vector for identification of ablated tumor was determined by correlation analysis between clustering-derived and histology-derived non-viable tumor fractions. To compare the multiparametric MRI analysis results with conventional HIFU monitoring and evaluation methods, the histology-derived non-viable tumor fractions were also quantitatively compared with non-perfused tumor fractions (derived from the level of contrast enhancement in the DCE-MRI measurements) and 240 EM tumor fractions (i.e. thermal dose > 240 equivalent minutes at 43°C, which is generally considered as a lethal thermal dose<sup>5</sup>).

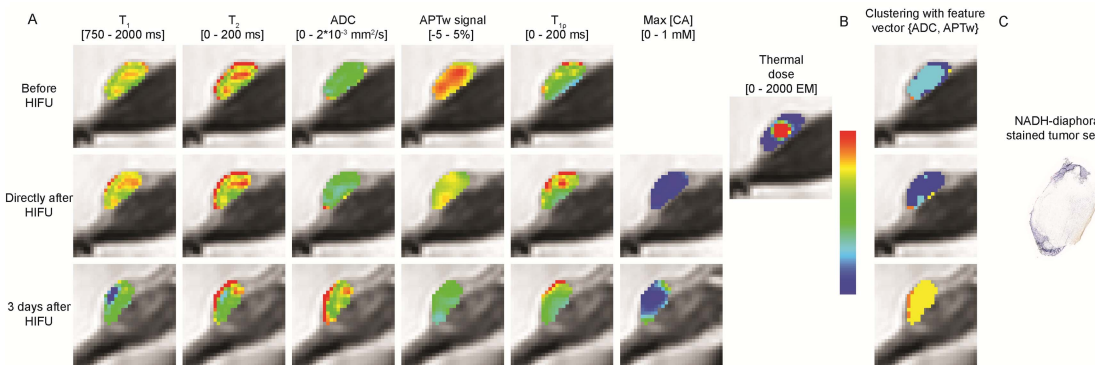


**Fig 1** A) Representative MRI parameter maps in the tumor tissue overlaid on  $T_2$ -weighted images. The max [CA] maps represent the maximum tissue contrast agent concentration derived from the DCE-MRI data. B) Results of k-means clustering with feature vector {ADC, APTw signal}. The different colors represent different clusters. The yellow and orange clusters were classified as non-viable. C) NADH-diaphorase stained tumor section obtained at 3 days after HIFU at approximately the same location as the shown MRI slice, showing a large region of pale, non-viable tumor tissue.

**Results** Representative MR parameter maps are shown in Fig 1 A. Changes in the individual MR parameter values after HIFU treatment were rather subtle and heterogeneous between the different endogenous contrast parameters. The maximum contrast agent concentration maps derived from the DCE-MRI measurements showed that the tumor was largely non-perfused directly after treatment, while the perfusion was partly restored at 3 days after treatment. The thermal dose map showed a circular region in which a high thermal dose was reached. Clustering with feature vector {ADC, APTw signal} resulted in distinct regions of tumor tissue classified as non-viable (consisting of the combined yellow and orange clusters) after HIFU treatment. These regions corresponded to non-viable tissue in histology (Fig 1 B/C). For this feature vector, a strong one-to-one correspondence ( $R^2$  to line of identity ( $R^2_{y=x}$ )=0.92 and strong correlation ( $r=0.92$ ) was observed between the histology-derived and clustering-derived non-viable tumor fractions when combining all groups. In Fig 2 A, B and C correlation plots between histology-derived and clustering-derived non-viable tumor fractions are shown for this particular feature vector for the individual groups (animals sacrificed directly after HIFU, at 3 days after HIFU and non-treated control animals, respectively). The correlation and one-to-one correspondence was largest at 3 days after HIFU treatment ( $R^2_{y=x}=0.97$ ,  $r=0.87$ , Fig 2 B). The correlation between histology-derived non-viable tumor fractions directly after HIFU and the 240 EM fractions was high, but not significant (Fig 2 D). The non-perfused fractions overestimated the extent of non-viable tumor tissue directly after HIFU treatment (Fig 2 E), while an underestimation was seen at 3 days after HIFU (Fig 2 F).

**Discussion and conclusion** We have shown that a multiparametric MR analysis, based on the ADC and the APT-weighted signal measured at 3 Tesla, can accurately determine the extent of non-viable tumor tissue after HIFU treatment. We expect that this method can be incorporated in the current clinical workflow of MR-HIFU ablation therapies.

**Acknowledgement** This research was supported by the Center for Translational Molecular Medicine (VOLTA).

**References** 1. Hectors et al. PloS One 2014;9(6):e99936, 2. Hectors et al. Magn Reson Med. 2014;72:1113-22, 3. Hectors et al. Magn Reson Med. 2014;doi:10.1002/mrm.25269, 4. Hijnen et al. Int J Hyperthermia 2012;28:2, 5. McDannold et al. Radiology 2000;216:517-523.

**Fig 2** Correlation plots between: histology-derived non-viable fractions and clustering-derived non-viable fractions for feature vector {ADC, APTw signal} for animals sacrificed directly after HIFU treatment (A), animals sacrificed 3 days after HIFU treatment (B) and non-treated control animals (C); histology-derived non-viable fractions and 240 EM fractions for animals sacrificed directly after HIFU (D); histology-derived non-viable fractions and DCE-MRI-derived non-perfused fractions directly after HIFU (E); histology-derived non-viable fractions and DCE-MRI-derived non-perfused fractions at 3 days after HIFU (F).

